Micromechanical Approach of Stress-Induced Phase Transformation

Etienne Patoor
Laboratoire de Physique et Mécanique des Matériaux (UMR CNRS 7554)
Ecole Nationale Supérieure d'Arts et Métiers, 4 rue Augustin Fresnel, Metz, France.

ABSTRACT

Stress-induced martensitic phase transformation is responsible of very important phenomena like superelasticity or two-way shape memory in shape memory alloys. These phenomena are at the origin of many innovative products in industrial fields like aerospace or biomedical applications. To reach the best design is a very difficult task for applications using shape memory alloys: due to the existence of a phase transformation, these materials can no longer be considered as homogeneous and macroscopic approaches failed to give an accurate description of their behavior. The recent trend using SMA thin film as microactuator in microdevice increase the need of reliable design tools. Moderns concepts developed in micromechanics and finite element analysis are well adapted to deal with these problems. Intra and intergranular stresses building from transformation strain incompatibilities in bulk materials or thin films are well accounted using these tools, even when complex loading conditions or different initial crystallographic texture are considered.

Keywords: Micromechanics, mechanical behavior, phase transition, shape memory alloys, thin film

1. INTRODUCTION

Modeling the functional behavior of shape memory alloys (SMA) is a challenge for the development of most of the industrial applications using these materials. Several works had established that concepts developed these last years in mechanics of materials like scale transition and homogenization methods, are very suitable to model the thermomechanical behavior of SMAs [1-4]. Strong predictive capacities are related to these approaches based upon a description of the strain mechanisms and where kinematical description and thermodynamical analysis are performed at a so-called microscopic level which is the pertinent scale to describe these mechanisms.

Due to its displacive character, the martensitic transformation is very sensitive to the stress state and internal stress field have to be taken into account for behavior modeling, these frameworks allow to give an estimation of the internal stress field building by strain incompatibilities. Two major sources of incompatibilities are found in SMAs. The first one deals with the nucleation and growth of several variants of martensite inside the parent phase crystal. The second is related to the granular structure of polycrystalline materials. Two successive homogenizations are then required considering the two representative scales involved. But numerical tools developed for dimensioning macro-components cannot be straightforward applied for micro-systems. To illustrate this point we consider the homogenization in bulk material with a self consistent approach and in thin film using a finite element code.

This paper is organized in three sections. In the first one we established the constitutive equations which govern the single crystal behavior. In the second one, an application of how the introduction of this behavior in a self consistent scheme allows to described the influence of the initial crystallographic texture on the macroscopic behavior of a bulk material is presented. In the third section we consider the case of thin film material and the single crystal constitutive law is now implemented into the FEM code ABAQUS via the UMAT (Users Material) routine. Results obtained for tensile test on a multicrystalline film are discussed and compared with those obtained for bulk material with a self-consistent approach.

etienne.patoor@metz.ensam.fr

Smart Structures and Materials 2003: Active Materials: Behavior and Mechanics,
Dimitris C. Lagoudas, Editor, Proceedings of SPIE Vol. 5053 (2003)
© 2003 SPIE · 0277-786X/03/$15.00

2. CRYSTALLOGRAPHIC DESCRIPTION OF THE SINGLE CRYSTAL BEHAVIOR

In scale transition scheme, the assumption of the existence of a Representative Volume Element (RVE) is a key point. To compute the overall response of polycrystalline materials, grains are very often chosen as RVE and kinematical and thermodynamical analysis are then performed at this scale, assuming that grains in polycrystal behave as single crystals.

2.1. Kinematical aspects

Let us considerd a Representative Volume Element (RVE), since for SMA, elastic constants may be approximated as identical in austenite and martensite and since plasticity can be neglected, only the stress free strain has to be specified for the martensitic transformation.

This transformation is a first order, non diffusive one. An inelastic lattice strain, the Bain strain, describes this geometrical transformation. It is usually strongly incompatible and a lattice invariant strain (LIS) must appear simultaneously. The LIS is deduced from compatibility conditions taking into account the observed morphology of the martensitic domains, using the Wechsler-Lieberman and Read Theory (WLR) [5] or the Eshelby inelastic inclusion problem [6]. The transformation strain ε^T, considered in this work as the stress free or inelastic strain in the sense of Eshelby [6] and Kröner [7], is the composition of the Bain strain and the LIS.

Let us consider the reference configuration of the RVE to be an austenitic stress free state. Thermomechanical loading transforms some part V_M of this RVE of volume V into martensite. The total deformation field $\varepsilon(r)$ results from several contributions: an elastic part denoted $\varepsilon^e(r)$, a thermal part $\varepsilon^{th}(r)$, the transformation part $\varepsilon^T(r)$, so that for the displacement field $u_i(r)$, one obtains:

$$u_{(i,j)} = \varepsilon_{ij}(r) = \varepsilon_{ij}^e(r) + \varepsilon_{ij}^{th}(r) + \varepsilon_{ij}^T(r) \tag{1}$$

where (i,j) means symetrisation of $u_{i,j}$. By integration over volume V under the assumption that, at ∂V, $u_i = E_{ij} x_j$, the overall mean deformation E_{ij} is given by :

$$E_{ij} = \frac{1}{V}\int_V \varepsilon_{ij}(r)dV = \frac{1}{V}\int_V \left\{\varepsilon_{ij}^e(r) + \varepsilon_{ij}^{th}(r) + \varepsilon_{ij}^T(r)\right\}dV \tag{2}$$

The overall strain E may be also decomposed into elastic (E^e) thermal (E^{th}) and transformation(E^p) parts.

If elastic compliances and thermal dilatations are assumed to be homogeneous, overall strains E^e and E^{th} can be identified with the corresponding mean values of their local parts, considering a uniform temperature field, one gets a global transformation strain E^T defined by:

$$E^T = \frac{1}{V}\int_V \varepsilon^T(r)dV \tag{3}$$

The field $\varepsilon^T(r)$ is piecewise uniform, keeping a uniform value ε^n inside each variant of martensite, one gets:

$$E_{ij}^T = \sum_n \varepsilon_{ij}^{Tn} f^n \quad \text{and} \quad f = \sum_n f^n \tag{4}$$

where parameters f^n represent the volume fraction of variants n and f denotes the global amount of martensite. In such a description, the transformation strain is a well-defined quantity and the volume fractions must satisfied the following physical constraints:

$$f^n \geq 0 \quad \text{for each } n \qquad \text{and} \qquad \sum_n f^n \leq 1 \tag{5}$$

Evolutions of these volume fractions with respects to the applied loading conditions, applied stress but also temperature variation, are defined through a thermodynamical analysis.

2.2. Thermodynamical potential and interaction energy

Thermodynamical potential over the RVE is composed by chemical, interfacial and elastic energies [3, 8]. Chemical energy depends to the temperature and to the volume fraction of martensite. A linear approximation around the equilibrium temperature is used. Interfacial energy is considered as negligible with respect to the other contributions, due to the oblate shape of martensite plates. The determination of the elastic energy is much more complex, because we have to consider the non uniformity in the transformation strain field associated to the nucleation and growth of several variants of martensite inside a same parent phase single crystal of volume V. Strain incompatibilities due to this microstructure built an internal stress field denotes by $\tau(r)$. The elastic energy is split into two contributions: one related to the applied stress σ and one, called the interaction energy, associated to the internal stress field [9,10].

$$W_{elas} = \frac{1}{2} \sigma_{ij} M_{ijkl} \sigma_{kl} - \frac{1}{2V} \int_V \tau_{ij}(r) \varepsilon^T_{ij}(r) \, dV \tag{6}$$

In equation 6, the four-order tensor M, denotes the elastic stiffness, which is assumed to be uniform in the two phases. According to micromechanical analysis [11, 12], the interaction energy, W_{int} can be approximated by a quadratic function of the volume fractions f^n of the different variant of martensite and requires the definition of an interaction matrix H^{nm} which gives the nature of the interaction (compatible or incompatible) between the different variants involved. The interaction energy by unit volume, may be expressed as:

$$W_{int} = -\frac{1}{2V} \int_V \tau_{ij}(r) \varepsilon^T_{ij}(r) \, dV = -\frac{1}{2V} \sum_n \bar{\varepsilon}^n_{ij} \bar{\tau}^n_{ij} V^n \tag{7}$$

where $\bar{\tau}^n$ and $\bar{\varepsilon}^n$ are average values of internal stress and transformation strain over the volume V^n occupied by a mixture of austenite and variant n. According to the works of Walpole [13] and Hill [14], across an interface between two domains n and m, having the same elastic constants, jumps in the stress and strain tensors are related by an interfacial operator, Q^{nm} which is a function to the normal of the interface and to the elastic constants:

$$\bar{\tau}^n_{ij} = \bar{\tau}^m_{ij} - Q^{nm}_{ijkl} \left(\bar{\varepsilon}^n_{kl} - \bar{\varepsilon}^m_{kl} \right) \tag{8}$$

From equations (7) and (8), interaction energy can be expressed as (with $F^n = V^n/V$) [12]:

$$W_{int} = -\frac{1}{2} \sum_{n,m} F^n F^m \left(\bar{\varepsilon}^n_{ij} - \bar{\varepsilon}^m_{ij} \right) Q^{nm}_{ijkl} \left(\bar{\varepsilon}^n_{kl} - \bar{\varepsilon}^m_{kl} \right) \tag{9}$$

From the observation that in polycrystalline material stress-induced transformation develops mainly two variants inside each grain, the minimization of the interaction energy is performed considering only interactions between couple of variants:

$$W_{int} \quad = \quad -\frac{1}{2} F^n F^m \left(\bar{\varepsilon}^n_{ij} - \bar{\varepsilon}^m_{ij}\right) Q^{nm}_{ijkl} \left(\bar{\varepsilon}^n_{kl} - \bar{\varepsilon}^m_{kl}\right) \tag{10}$$

Minimization of expression (10) for every couple of two variants allows defining a 24x24 interaction matrix taking into account all the possible interactions between two variants. Two kinds of interaction are obtained: compatible interaction when the minimum value takes by W_{int} is close to zero and incompatible one, when this value is large. This determination is very suitable for Cu-based shape memory alloys and gives good agreement when it is introduced into a self-consistent scheme to compute the overall behavior of these alloys. At the crystal scale, the four-variants self-accommodating groups experimentally observed are also determined in that way for CuZnAl and CuAlBe alloys. This interaction matrix was introduced in several crystallographical approaches [4, 15].

	1	2	3	4	5	6	7	8	9	10	11	12	13	14	15	16	17	18	19	20	21	22	23	24
1	▨	▨	▨	▨	▨			▨				▨				▨	▨							▨
2	▨	▨	▨✕	▨		▨	▨	✕			▨				▨			▨					▨	
3	▨	▨✕	▨	▨		▨	▨	✕		▨				▨					▨			▨		
4	▨	▨	▨	▨	▨			▨	▨				▨							▨	▨			
5	▨			▨	▨	▨	▨	▨				▨				▨				▨	▨			
6		▨	▨		▨	▨	▨	▨			▨				▨				▨			▨		
7		▨	▨		▨	▨	▨	▨		▨				▨				▨					▨	
8	▨	✕	✕	▨	▨	▨	▨	▨	▨				▨				▨							▨
9				▨				▨	▨	▨	▨	▨	▨			▨		▨				▨		
10			▨				▨		▨	▨	▨	▨		▨	▨		▨				▨			
11		▨				▨			▨	▨	▨	▨		▨	▨					▨				▨
12	▨				▨				▨	▨	▨	▨	▨			▨			▨				▨	
13				▨				▨	▨			▨	▨	▨	▨	▨			▨				▨	
14			▨				▨			▨	▨		▨	▨	▨	▨				▨				▨
15		▨				▨				▨	▨		▨	▨	▨	▨	▨				▨			
16	▨				▨				▨			▨	▨	▨	▨	▨		▨				▨		
17	▨							▨		▨					▨		▨	▨	▨	▨	▨			▨
18		▨					▨		▨							▨	▨	▨	▨	▨		▨	▨	
19			▨			▨						▨	▨				▨	▨	▨	▨		▨	▨	
20				▨	▨						▨			▨			▨	▨	▨	▨	▨			▨
21				▨	▨						▨				▨		▨			▨	▨	▨	▨	▨
22			▨			▨						▨				▨		▨	▨		▨	▨	▨	▨
23		▨					▨		▨				▨					▨	▨		▨	▨	▨	▨
24	▨							▨		▨				▨			▨			▨	▨	▨	▨	▨

Table 1. Interaction matrix for Cu-based SMAs, gray boxes means compatibility between two variants [12].

According to this definition of the interaction matrix H, the interaction energy (7) writes then as:

$$W_{int} = \frac{1}{2} \sum_{n,m} H^{nm} f^n \; f^m \tag{11}$$

It is necessary to note that the assumptions used to determine this matrix limit its utilization to stress-induced transformations (superelasticity and two-way shape memory). Among these limitations, the number of variants present in a grain has to remain weak. By consequence, in a fully thermally-induced martensitic state where different self-accommodated groups coexist the use of this matrix gives a considerable overestimation of the elastic energy associated to this configuration. An extension of this work for the martensitic state was recently proposed by Niclaeys et al. [16].

2.3. Thermodynamical forces and crystal behavior law

Utilization of relationship (11) in the free energy allows to use only the volume fraction of the different variants of martensite as internal variables:

$$\Psi(\Sigma_{ij},T,f^n) = \frac{1}{2}\Sigma_{ij}\,M_{ijkl}\,\Sigma_{kl} + \Sigma_{ij}\,\varepsilon_{ij}^n\,f^n - \frac{1}{2}\sum_{n,m} H^{nm}\,f^n\,f^m - B(T-T_0)\sum_{n} f^n \qquad (12)$$

The partial derivatives of potential (12), with respect to physical constraints (5) allows to define the thermodynamical forces $\mathcal{F}^n$ acting on internal variables f^n . Lagrange multipliers λ_0 and λ_n are associated to these constraints [10].

$$\mathcal{F}^n = \Sigma_{ij}\,\varepsilon_{ij}^n - \sum_{m} H^{nm}\,f^m - B(T-T_0) - \lambda_0 + \lambda_n \qquad (13)$$

Due to the existence of hysteresis phenomena, the knowledge of thermodynamical forces (13) is not enough to derive the thermomechanical behavior associated to a stress-induced martensitic transformation. Hysteresis is linked to dissipation process occurring during the transformation so we introduce a dissipative potential W^d. Evolution of this potential has to respect the second principle of thermodynamic. Combined utilization of this fundamental law with the energy balance gives:

$$\dot{\Psi}\,\big|_{\Sigma,\,T} = \dot{W}^d \geq 0 \qquad (14)$$

Like in plasticity, one supposes that the thermodynamical driving force has to reach a critical value to produce growth (or shrinkage) on a variant. This value is assumed to be a positive material constants, $\mathcal{F}_c$, identical for all the variants. With this hypothesis the dissipative potential turns to be a function proportional to the cumulative volume fraction f_{cu} of martensite [10].

$$W^d = \mathcal{F}_c \int_0^t \left|df\right| = \mathcal{F}_c\,f_{cu} \qquad (15)$$

This analysis allows to define local transformation criteria. A volume of austenite transforms to a given variant of martensite when:

$$\Sigma_{ij}\,\varepsilon_{ij}^n - \sum_{n} H^{nm}\,f^m - B(T-T_0) + \lambda_n - \lambda_0 = \mathcal{F}_c \qquad (16)$$

Nevertheless, the transformation only occurs if the Lagrange multipliers λ_n and λ_0 are positive or null quantities:

$$\lambda_n = -\Sigma_{ij}\,\varepsilon_{ij}^{n} + \sum_{n} H^{nm} f^{m} + B(T - T_0) + \lambda_0 + \mathcal{F}_c \geq 0$$

$$\lambda_0 = \Sigma_{ij}\,\varepsilon_{ij}^{n} - \sum_{n} H^{nm} f^{m} - B(T - T_0) + \lambda_n - \mathcal{F}_c \geq 0 \tag{17}$$

These restrictions constitute a major difference from the modeling of plastic behavior by dislocations motion. Conditions (16) and (17) constitute the local criteria for thermoelastic martensitic transformation. If these conditions are satisfied, utilization of the coherency rule allows to determine evolution of the transformation rates on each variants:

$$\dot{F}^n = \frac{\partial \dot{F}^n}{\partial \Sigma_{ij}}\dot{\Sigma}_{ij} + \frac{\partial \dot{F}^n}{\partial T}\dot{T} + \sum_{m} \frac{\partial \dot{\mathbf{F}}^n}{\partial f^m}\dot{f}^m = 0 \tag{18}$$

Substitution of driving force (13) gives :

$$\varepsilon_{ij}^{n}\,\dot{\Sigma}_{ij} - B\,\dot{T} - \sum_{m} H^{nm}\,\dot{f}^{m} = 0 \tag{19}$$

Resolution of this system equation gives the transformation with respects to the loading parameters. Using this result into the kinematical equation (4) defines the constitutive equation for the single crystal behavior.

$$\dot{E}_{ij}^{T} = \sum_{n} \varepsilon_{ij}^{n} \sum_{m} \left(H^{nm}\right)^{-1} [\varepsilon_{kl}^{m}\,\dot{\Sigma}_{kl} - B\,\dot{T}] \tag{20}$$

This equation characterizes the behavior of a unit volume crystal of parent phase undergoing a stress-induced martensitic transformation. Production of several variants of martensite is taken into account. This polyvariants transformation difficult to produce in single crystal happens in the grains of polycrystalline material. Relationship (4) is now used in the next to section to describe the local behavior at the grain level in scale transition approach using a self consistent framework for the bulk and a finite element code for a thin film.

3. POLYCRYSTALLINE BEHAVIOR IN BULK MATERIAL

In polycrystalline material incompatibility in the strain field comes from the granular structure . Bhattacharya & Kohn [17] have underlined the effect of texture on the occurrence of the SMA effect. In this paper we use a self-consistent approximation to compute the overall response. In this scheme, the transformation mechanism is defined at the RVE scale (see previous section). To describe the granular structure, each grain is represented by its shape, volume fraction and crystallographic orientation, given by the three Euler's angles [10]. In this section we address the shape of transformation surface in the stress space as a function of initial texture and we compare the effect of three different one on a CuZnAl alloys.

The shape of the transformation surface is a important feature for the mechanical behavior. Behavior laws used in structure calculation code are based upon transformation criterion defined from these surface [18]. In order to determine the influence of the initial crystallographical texture we compute it for an isotropic texture having a random distribution of the grains orientation, a rolling one and a drawing one. In these last two cases, initial orientation of grains is rotated by a 50% plastic strain.

For these three textures the transformation surface is defined at the same strain level, varying the loading direction (figure 1), 140 different loadings are compute for each surface. For all textures there is no symmetry according to the tension or compression tests. Important shape changes were observed according to the initial crystallographic texture. This clearly indicates that the orientation of austenitic grains strongly influence the way the different grains transform and by consequence the kinetics of the martensitic transformation. This kind of analysis allows the optimization of the texture according to the loading conditions imposed.

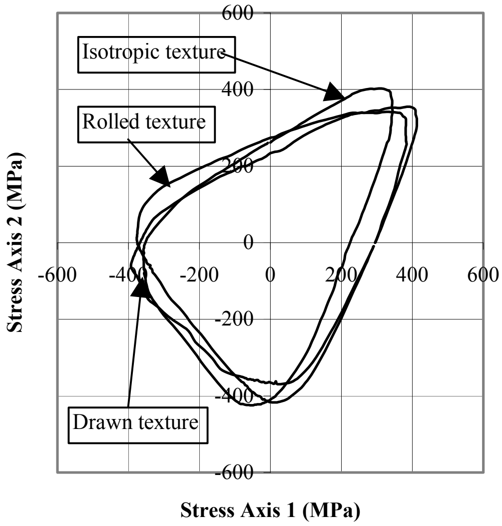

Figure 1: Influence of the initial crystallographic texture on the transformation surface defined at 0.4 % transformation strain for a CuZnAl superelatic alloys (M_s = -100 C).

4. APPLICATION TO A MULTICRISTALLINE FILM

Numerical tools developed for dimensioning macro-components cannot be straightforward applied for micro-systems. In this case, scale transition scheme must take into account that grain size is of the same order of magnitude as the component itself so the notion of equivalent homogeneous material is no longer valid. In addition, surface effects are now very important. The Finite Elements Method (FEM) is well adapted to deal with grain shape, grain size and also the relative position of each grain with respect to the film surface.

In the third part of this paper, the single crystal constitutive law for the superelastic behavior of SMA is implemented into the FEM code ABAQUS via the UMAT (Users Material) routine. Results obtained for tensile test on a multicrystalline film are discussed and compared with those obtained for bulk material with a self-consistent approach.

4.1 Geometrical description and boundary conditions

We consider a plate structure composed with six grains having one grain in the thickness (figure 2). A 10x5x0.1 mm CuAlBe superelastic SMA plate is meshed. Each grain are described with 144 isoparametric tridimensionnal elements [19]. Euler angles and the Schmid factor (R_{11}) in the longitudinal direction are given in table 2.

	φ1	φ	φ2	R_{11}
Grain # 1	351.9	21.3	212.1	0.49
Grain # 2	173.4	104.5	34.5	0.43
Grain # 3	88.6	55.6	327.6	0.4
Grain # 4	210.3	91.9	131.8	0.21
Grain #5	21.6	127.7	56.96	0.33
Grain # 6	234.4	148.3	268.5	0.28

Table 2. Crystallographical orientation (Euler angles φ^1, φ, φ^2) and Schmid factor for a longitudinal tensile test for each grain.

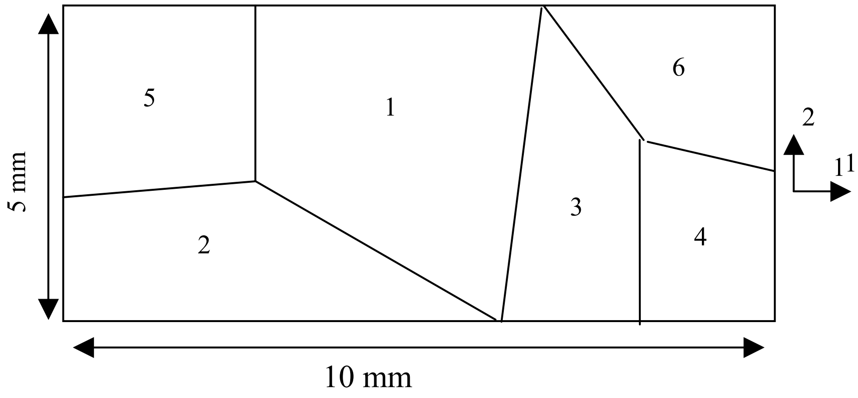

Figure 2: Representation of the geometry adopted for the thin film

From data in table 2 we observed that grain # 1 is the best oriented with respect to the longitudinal loading direction. In the opposite grain # 4 has the smallest Schmid factor. We simulated a tensile test along the longitudinal direction 1. Boundary conditions, loading and meshing are represented in figure 3. We imposed the following boundary conditions:

- All the nodes of the left face are blocked in direction 1, a node of this face is blocked in directions 2 and 3.
- All the nodes of the right face are submit to a displacement according to direction 1.

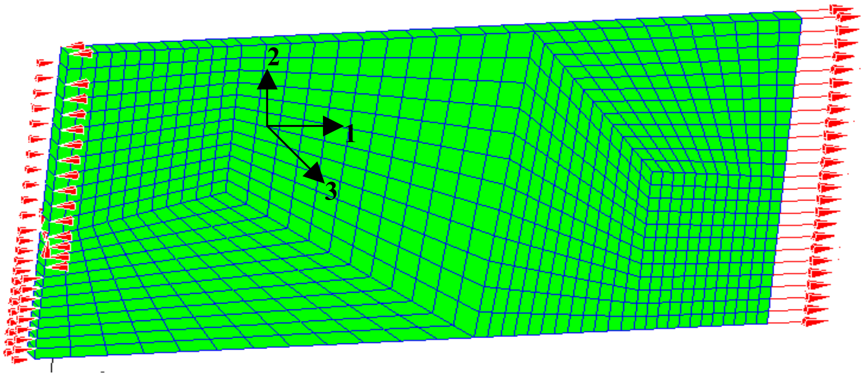

Figure 3. Representation of boundary conditions applied and the meshing of the plate

4.2 Martensite volume fraction

This model allows to determine the evolution of the martensite volume fraction during the loading sequence. The first variant of martensite appears in grain # 1. The last grain where the transformation takes place is logically grain # 4. This sequence is in good agreement with experimental features. A very large intergranular heterogeneity is observed for the volume fraction of martensite (figure 4). When grain # 1 is almost fully martensitic (92 % martensite), grain # 4 is still almost austenitic (only 4 % martensite) and the global average volume fraction for the structure reaches 50%.

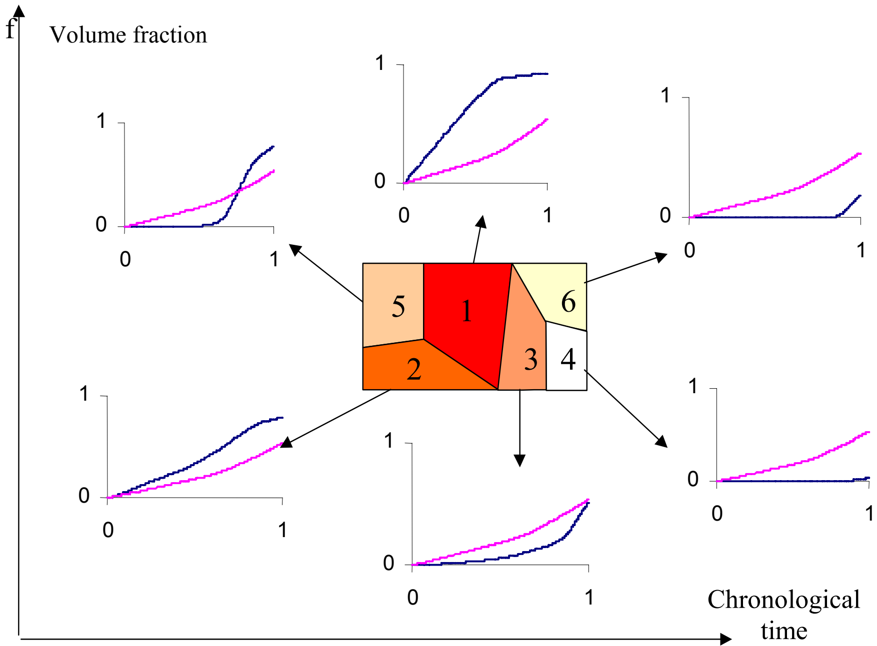

Figure 4. Evolution for each grain of the volume fraction during the loading sequence

4.3 Thin film effect

This heterogeneity in volume fraction is also observed on the mechanical behavior. On figure 5, stress-strain curves for each grain are plotted and compared with the macroscopic response. We observed than grain # 1 first easily transforms at the beginning of the loading and its transformation strain saturates as the transformation progresses in the adjacent grains. This transition is related to a strong inflexion on the macroscopic curve. We also observe that for the other grains, stress-strain curves have a more complex shape that can be related to the formation of several different variants of martensite inside these grains.

The strong influence on the surrounding on the grain individual behavior can be underline if we compare the behavior exhibit by a grain inside a thin film with the stress-strain curve determined for a grain having the same crystallographic orientation and the same elastic and phase change properties but embedded in a bulk polycrystalline structure. Curves; presented in figure 6 are computed using the self consistent scheme used in the previous section. We consider an aggregate composed with 106 spherical grains with an isotropic crystallographical texture and the constitutive behavior defined in equation (21). The longitudinal direction of the thin film is kept as the tension loading axis for the bulk material. So every parameters are kept constant, only the internal stress field which is directly associated to how strain incompatibilities are developed during the phase transformation can change.

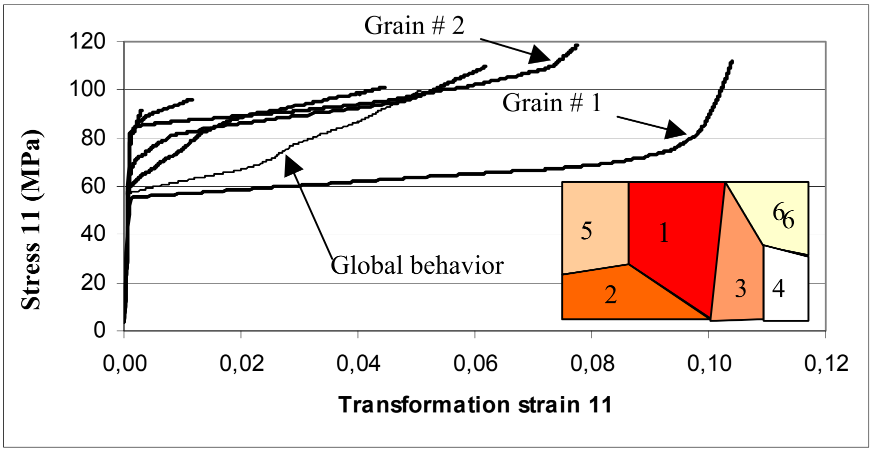

Figure 5. FEM determination of stress-induced curves grains in thin film

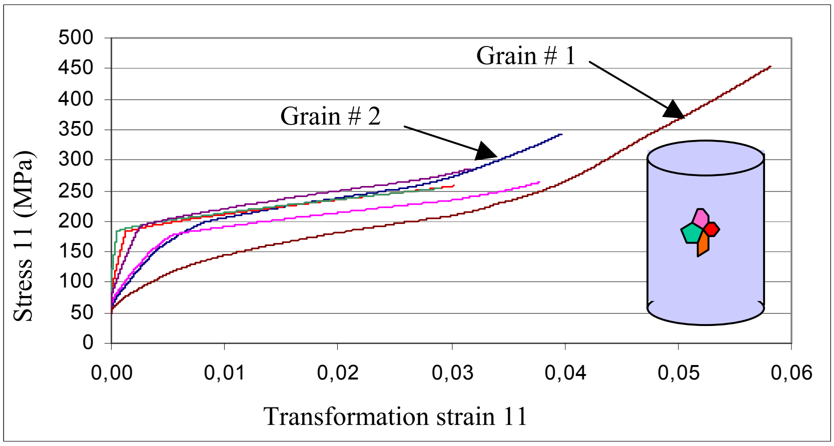

Figure 6. Stress-strain curves computed using a self-consistent code for grains having the same crystallographic orientation as in table 1 but embedded in a bulk material

Comparison between the stress-strain curves in figures 5 and 6 undoubtedly establish the leading influence of the internal tress field on the way the phase transformation proceeds in a given grain. If we consider, inside the bulk material, a grain having the same well-oriented crystallographic direction as grain #1, we observed that this grain is only partially transformed and this despite a stress level now four time higher than in the thin film. In figure 5, the transformation strain for grain # 1 reaches 10% at 100 MPa and in figure 6, at the same test temperature, this transformation strain is now lower than 6% but the stress exceeds 400 MPa. Similar observations can be made on other grains like grain # 2 for instance.

5. CONCLUSION

In this work a crystallographical description of the single crystal behavior law for superelasticity in SMA was successfully implemented in a self consistent approach and in the finite element code ABAQUS. This last approach is well adapted to compute the mechanical response of thin film. Crystallographical orientation, grain shape, grain size and surface effect are accounted in that way. Experimental validation is under way using EBSD and X-ray diffraction techniques. Comparison with the self-consistent simulation establishes the major influence of the surrounding on the way the transformation proceed in an austenitic crystal for a given crystallographic orientation.

REFERENCES

1. Ono, N. and Sato, A., "Plastic deformation governed by the stress induced martensitic transformation in polycristals". *Trans. Japan Inst. of Metal,* **29**, 267-273, 1988.
2. Sun, Q.P. and Hwang, K. C., "Micromechanical modelling for the constitutive behavior of polycrystalline shape memory alloys, I and II". *J. Mech. Phys. Solids*, **41**, 1-17 and 19-33, 1993.
3. Patoor, E., Eberhardt, A. and Berveiller, M., "Thermomechanical behaviour of shape memory alloys". *Arch. of Mech*., **40**, 775-794, 1988.
4. Gall, K and Sehitoglu, H., "The role of texture in tension-compression asymmetry in polycrystalline NiTi", *International Journal of Plasticity*, **15**, 69-92, 1999.
5. Weschler, M.S., Lieberman, D.S. and Read, T.A., "On the theory of the formation of martensite", *Transaction of AIME*, **197**, 1503-1515, 1953.
6. J.D. Eshelby, in Progress in Solids Mechanics, (Ed. I.N. Sneddon, R. Hill), Vol. 2, North-Holland, Amsterdam, pp. 87-140, 1961.
7. E. Kröner, Acta metall., **9**, 155-161, 1961.
8. Ortin, J. and Planes, T., "Thermodynamics analysis of thermal measurements in thermoelastic martensitic transformations". *Acta metall*., **36**, 1873-1889, 1988.
9. Mura, T., *Micromechanics of defects in solids*. Martinus Nijhoff, The Hague, 1987.
10. Patoor, E. and Berveiller, M., "Micromechanichal modelling of thermomechanical behavior of shape memory". *In CISM Lecture Notes, **368**, 121-188*, eds. F.D. Fisher & M. Berveiller, Springer Wien New York, 1997.
11. Fassi Fehri, O., Hihi, A. and Berveiller, M. , "Elastic interactions between variants in pseudoelastic single crystals". *Scripta Met.* **21**, 771, 1987.
12. Siredey, N., Patoor, E., Berveiller and Eberhardt, A., "Constitutive equations for polycrystalline thermoelastic shape memory alloys. Part I. Intragranulaire interactions and behavior of the grain", *International Journal of Solids and Structures*, **36**, 4289-4315, 1999.
13. Walpole, L.J., "The elastic field of an inclusion in an anisotropic medium". *P. Roy. Soc. Lond. A Mat., **300**,* 270-289, 1967.
14. Hill, R., "Interfacial operators in the mechanics of composite media", *J. Mech. Phys. Solids,* **31***,* 347-357, 1983.
15. Gao, X., Huang, M. and Brinson, C., "A multivariant micromechanical model for SMAs. Part I. Crystallographic issues for single crystal model". *International Journal of. Plasticity*, **16**, 1345-1369, 2000.
16. Niclaeys C, Ben Zineb T., Arbab Chirani S, Patoor E., "Determination of the interaction energy in the martensitic state", International Journal of Plasticity, **18**, 1619-1647, 2002.
17. Bhattacharya, K and Kohn, R.V, "Symmetry, Texture and the Recoverable Strain of Shape Memory Polycrystals", *Acta mater*., **44**, 529-542, 1996.
18. Gillet, Y., Patoor, E. and Berveiller, M., "Calculation of pseudoelastic elements using a non-symetrical thermomechanical transformation criterion and associated rule", *Journal of intelligent material systems and structures*, **9**, 366-378, 1998.
19. Niclaeys C, Thesis, Metz University, "Comportement des monocristaux en AMF. Application au comportement des polycristaux", 2002.